

Supporting Information

Construction of 9, 9'-Bifluorenylidene-based Small Molecule Acceptor Material by Screening Conformation, Steric Configuration and Repeating Unit Number: A Theoretical Design and Characterization

Ming-Yue Sui,^a Yun Geng,^b Guang-Yan Sun,^{a} Jian-Ping Wang^{c*}*

^a Department of Chemistry, Faculty of Science, Yanbian University, Yanji, Jilin, 133002, China. *E-mail: gysun@ybu.edu.cn

^b Institute of Functional Material Chemistry, Faculty of Chemistry, Northeast Normal University, Changchun, Jilin, 130024, China.

^c Shaanxi Key Laboratory of Natural Products & Chemical Biology, College of Chemistry & Pharmacy, Northwest A&F University, Yangling, Shaanxi, 712100, China. *E-mail: wangjp304@nwsuaf.edu.cn.

Section S.1. Computational Details of Marcus Rate Parameters

S.1.1 Reorganization Energy

The total reorganization energy λ includes internal reorganization energy (λ_{int}) and external reorganization energy (λ_{ext}).¹ The λ_{int} derive from the changes in the ground-state structures of D and A when they gain or lose charge upon electron transfer, which is expressed as:²

$$\lambda_{\text{int}} = \left[E(A^-) - E(A) \right] + \left[E(D) - E(D^+) \right] \quad (\text{E.1})$$

where $E(A^-)$ and $E(A)$ are the energies of the neutral acceptor A at the anionic and optimal ground-state geometries, respectively. $E(D^+)$ and $E(D)$ are the energies of the cation donor D at the neutral and optimal cation geometries, respectively.

However, the λ_{ext} is due to electronic and nuclear polarization from the surrounding medium, which can be approximately evaluated by:³

$$\lambda_{\text{ext}} = \frac{1}{4\pi\epsilon_0} \Delta e^2 \left(\frac{1}{2a_1} + \frac{1}{2a_2} - \frac{1}{R} \right) \left(\frac{1}{\epsilon_{\text{OP}}} - \frac{1}{\epsilon_0} \right) \quad (\text{E.2})$$

where a_1 , a_2 , R , ϵ_{OP} , and ϵ_0 are donor radii, acceptor radii, the distance between the center of the donor and acceptor, and optical and the zero-frequency dielectric constants of the surrounding media, respectively. Considering the reconciliation between the computational cost and the accuracy, ϵ_{OP} and ϵ_0 is estimated to be 1.96 and 5 by Troisi⁴ and Jérôme¹, respectively.

S.1.2 Electronic Coupling

For the calculation of inter-CT and inter-CR rates, the electronic coupling can be approximated from the generalized Mulliken-Hush (GMH) formalism^{5,6} in adiabatic description, which could be written as below:

$$V_{\text{DA}} = \frac{\mu_{\text{tr}} \Delta E}{\sqrt{(\Delta\mu)^2 + 4(\mu_{\text{tr}})^2}} \quad (\text{E.3})$$

where μ_{tr} is the average transition dipole moment, $\Delta\mu$ is the dipole moment difference between initial state S_0 and final state S_n , and ΔE corresponds to the vertical excitation energy. The $\Delta\mu$ can be estimated directly from a finite field method on the excitation energy.²

S.1.3 Gibbs Free Energy

In the interface charge transfer processes, Gibbs free energy change of charge recombination ($\Delta G_{inter-CR}$) can be expressed under the equation:⁷

$$\Delta G_{CR} = E_{IP}(D) - E_{EA}(A) \quad (E.4)$$

where $E_{IP}(D)$ is the ionization potential of the donor which could be estimated by the HOMO energy of the donor, and $E_{EA}(A)$ is the electron affinity of the acceptor which is considered to be the LUMO energy of the acceptor here.⁸

The Gibbs free energy change of exciton dissociation ($\Delta G_{inter-CS}$), can be evaluated by the Rehm-Weller equation:⁷

$$\Delta G_{CS} = -\Delta G_{CR} - \Delta E_{0-0} - E_B \quad (E.5)$$

Where ΔE_{0-0} is the lowest excited state energy of free-base donor and E_B is the exciton binding energy, defined as the energy difference between the electronic and optical band-gap energy.⁹

Tables:

Table S1. Calculated and experimental bond lengths (in Å), bond angles (in deg) and torsion angles (in deg) of the configuration **c** for 99'BF at S_0 state (B3LYP/6-31G(d)).

c					
	Cal.	Exp. ^a		Cal.	Exp. ^a
	Bond Length (Å)		Bond Angle (deg)		
R(1,10)	1.400	1.397	A(10,9,13)	105.4	104.9
R(1,2)	1.397	1.399	A(9,10,11)	109.0	109.1

R(2,3)	1.399	1.371	A(10,11,12)	108.3	108.4
R(3,4)	1.397	1.373	Torsion Angle (deg)		
R(4,11)	1.393	1.394	DA(10,9,9',10')	34.0	34.0
R(9,10)	1.482	1.476			
R(10,11)	1.419	1.400			
R(11,12)	1.463	1.454			
R(9,9')	1.381	1.367			

a) Abbreviations: R = bond length, A = bond angle, DA = torsion angle.

^a Data from reference [22, 68].

Table S2. Calculated The FMO energy level (eV) for the P3HT (n=6) derivatives at the B3LYP/6-31G(d) level.

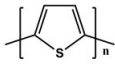
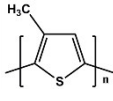
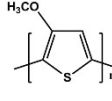
n=6	6T: 	P3HT(-CH3): 	P3HT(-OCH3): 
HOMO	-4.82	-4.98	-4.12
LUMO	-2.15	-1.67	-1.77
E_g	2.67	3.31	2.35

Table S3. Calculated bond lengths (in Å), bond angles (in deg) and torsion angles (in deg) of the configuration **p** for 99'BF at S_0 state (B3LYP/6-31G(d)).

p				
	Bond Length (Å)		Bond Angle (deg)	
R(1,10)	1.398	A(10,9,13)	103.60	
R(1,2)	1.399	A(9,10,11)	108.50	
R(2,3)	1.397	A(10,11,12)	108.30	
R(3,4)	1.397	Torsion Angle (deg)		
R(4,11)	1.393	DA(10,9,9',10')	-9.51	
R(9,10)	1.497			
R(10,11)	1.418			
R(11,12)	1.464			
R(9,9')	1.375			

Table S4. Calculated maximum absorption peaks λ_{\max} (nm), oscillator strengths f and major configurations of the **p** derivatives at the TD-B3LYP/6-31G(d) level.

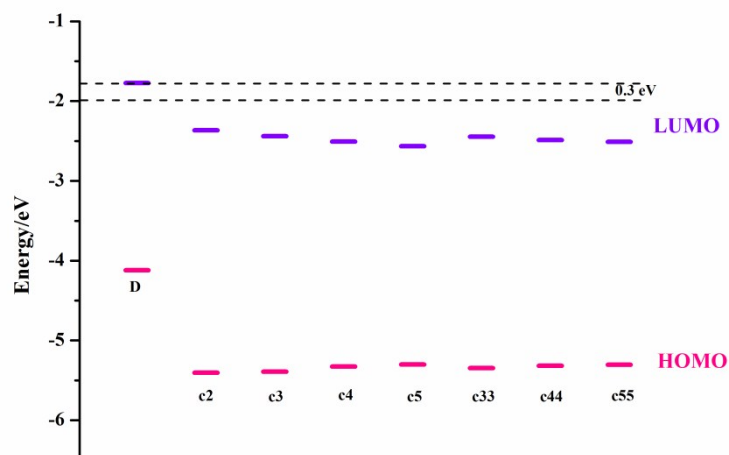
	states	λ_{\max}	f	composition	
p2	S_1	466.7	0.695	H→L (85%)	H-2→L (9%)
	S_5	424.5	0.481	H-4→L (15%)	H-2→L (53%)
p3	S_2	467.1	1.046	H→L (90%)	H-1→L+1 (3%)

	S_9	415.8	0.435	H-1→L+1 (47%)	H-1→L+2 (7%)
p4	S_1	501.1	1.613	H→L (92%)	
p5	S_1	513.8	1.990	H→L (96%)	
p33	S_1	490.4	1.492	H→L (90%)	H-1→L+1 (3%)
	S_7	432.2	0.341	H-6→L (33%)	H-4→L (23%)
p44	S_1	503.9	2.244	H→L (88%)	H-1→L+1 (6%)
p55	S_1	511.2	2.942	H→L (82%)	H-1→L+1 (10%)

Table S5. Computed internal reorganization energy λ_{int} (eV), external reorganization energy λ_{ext} (eV), total reorganization energy λ (eV), gibbs free energy change ΔG (eV) and electronic coupling V_{DA} (eV) of D/p**2-p55** at the TD-CAM-B3LYP/6-31G(d)//B3LYP/6-31G(d) level.

	λ_{int}	λ_{ext}	λ	V_{DA}	ΔG_{CS}	ΔG_{CR}
D/c 2	0.27	0.21	0.47	5.61	-0.91	-1.44
D/c 3	0.23	0.19	0.42	4.68	-0.97	-1.38
D/c 4	0.23	0.17	0.40	3.87	-1.04	-1.31
D/c 5	0.23	0.17	0.40	3.34	-1.09	-1.26
D/c 33	0.23	0.17	0.40	2.29	-0.99	-1.36
D/c 44	0.22	0.15	0.37	5.01	-1.02	-1.33
D/c 55	0.20	0.15	0.35	4.56	-1.05	-1.30
D/p 2	0.27	0.21	0.48	7.63	-1.76	-0.59
D/p 3	0.23	0.19	0.42	2.65	-1.68	-0.67
D/p 4	0.23	0.17	0.40	3.87	-1.61	-0.74
D/p 5	0.23	0.17	0.40	5.22	-1.56	-0.79
D/p 33	0.24	0.17	0.41	2.18	-1.68	-0.67
D/p 44	0.22	0.15	0.37	1.39	-1.63	-0.72
D/p 55	0.20	0.15	0.35	3.97	-1.61	-0.74

Figures:



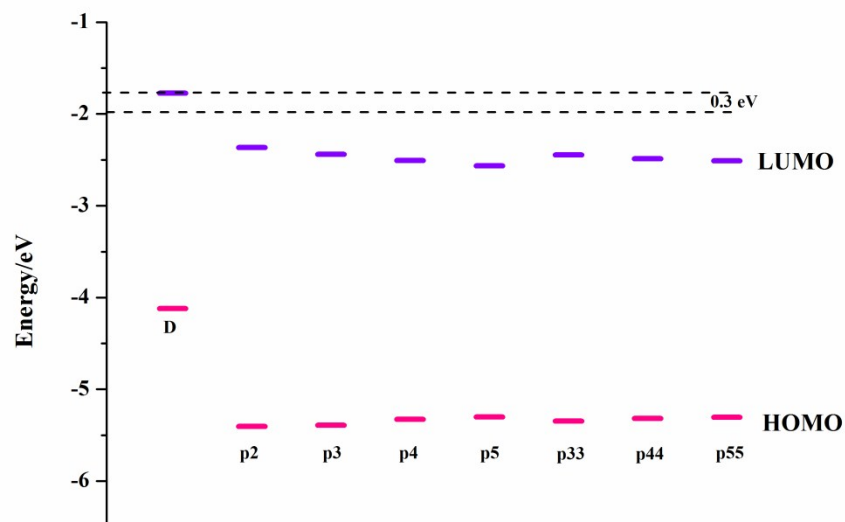


Figure S1. Illustration of FMO energy levels for the studied compounds and donor (D) evaluated at the B3LYP/6-31G(d) and TD-B3LYP/6-31G(d) levels.

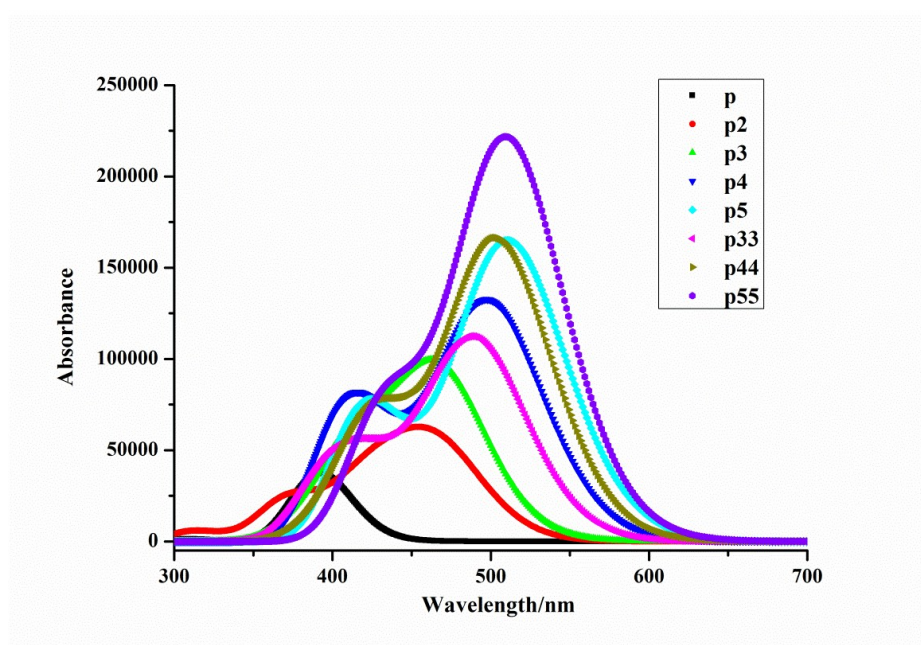


Figure S2. Simulated absorption spectra of the **p** derivatives at the TD-B3LYP/6-31G(d) level.

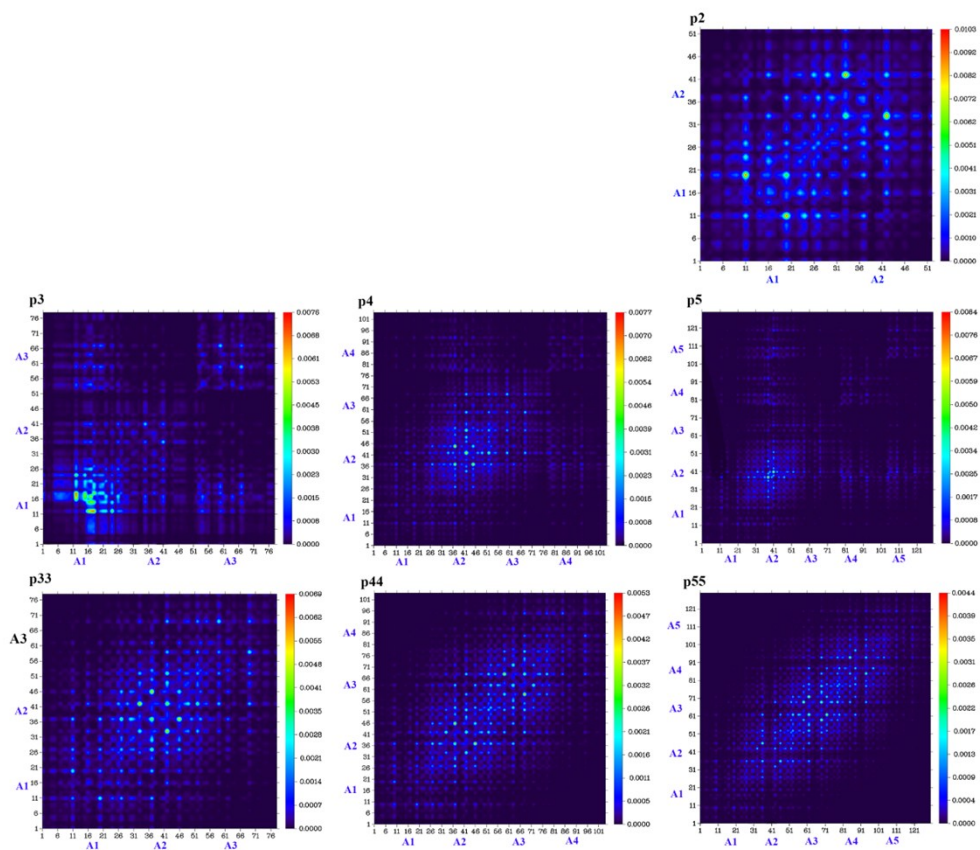


Figure S3. Simulated transition density matrix (TDM) associated with the lowest excited states of p2-p55 (the hydrogen atoms of all systems are omitted), and the color bars are given on the right.

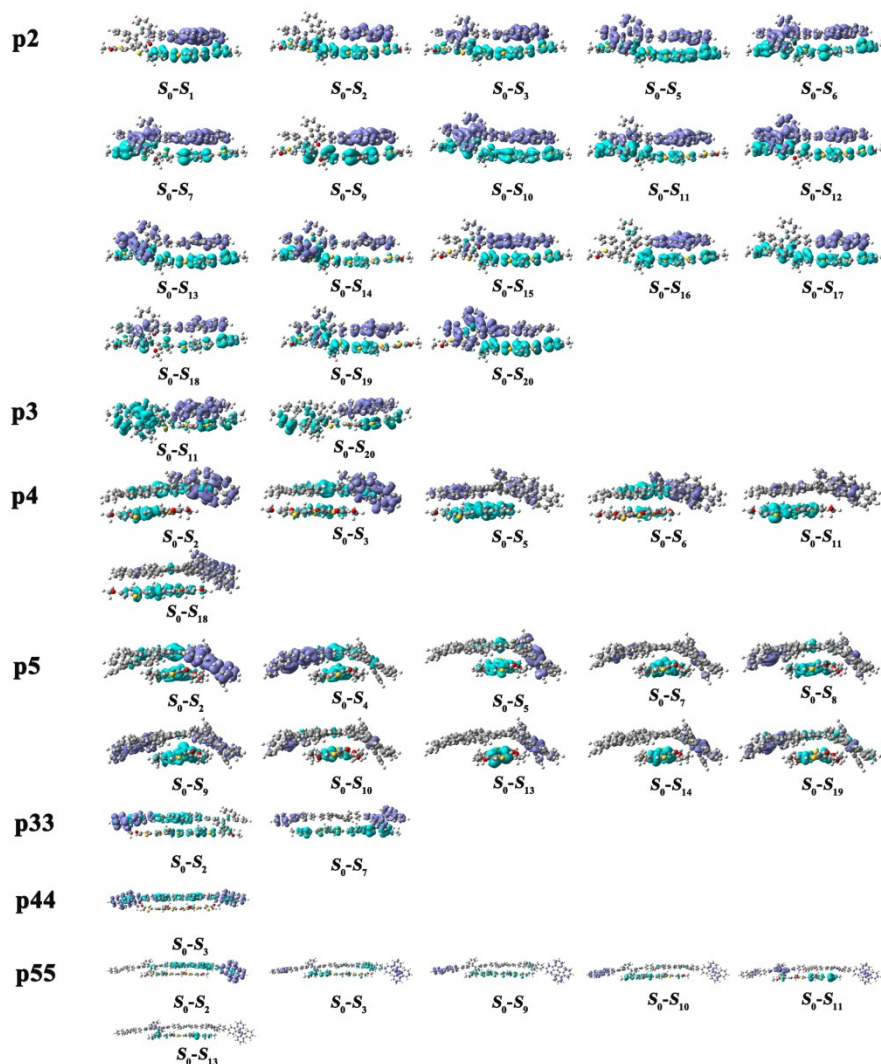


Figure S4. Charge density difference maps of inter-CT excited states for D/p2-p55 heterojunctions at the TD-CAM-B3LYP/6-31G(d)//B3LYP/6-31G(d) level, where the violet and turquoise colors stand for the increase and decrease in electron density, respectively.

References:

- 1 Lemaur, V.; Steel, M.; Beljonne, D.; Brédas, J. L.; Cornil, J., *J. Am. Chem. Soc.* **2005**, *127*, 6077-6086.
- 2 Li, Y.; Pullerits, T.; Zhao, M.; Sun, M., *J. Phys. Chem. C* **2011**, *115*, 21865-21873.
- 3 Marcus, R. A., *J. Chem. Phys.* **1956**, *24*, 966-978.
- 4 Liu, T.; Troisi, A., *J. Phys. Chem. C* **2011**, *115*, 2406-2415.

- 5 Voityuk, A. A., *J. Chem. Phys.* **2006**, *124*, 064505.
- 6 Hsu, C.-P., *Acc. Chem. Res.* **2009**, *42*, 509-518.
- 7 Kavarnos, G. J.; Turro, N. J., *Chem. Rev.* **1986**, *86*, 401-449.
- 8 Zhang, X.; Chi, L.; Ji, S.; Wu, Y.; Song, P.; Han, K.; Guo, H.; James, T. D.;
Zhao, J., *J. Am. Chem. Soc.* **2009**, *131*, 17452-17463.
- 9 Scholes, G. D.; Rumbles, G., *Nat. Mater.* **2006**, *5*, 683-696.